GeoResJ 7 (2015) 59–65

Contents lists available at ScienceDirect

GeoResJ

journal homepage: www.elsevier.com/locate/GRJ

An outlet for Pacific mantle: The Caribbean Sea?

Rainer Nerlich [a,b,*], Stuart R. Clark [b,1], Hans-Peter Bunge [a,2]

[a] Department of Earth and Environmental Sciences, Geophysics, Munich University, Theresienstr. 41, 80333 Munich, Germany
[b] Kalkulo AS, Simula Research Laboratory, P.O. Box 134, 1325 Lysaker, Norway

ARTICLE INFO

Article history:
Received 15 January 2015
Revised 3 June 2015
Accepted 3 June 2015
Available online 21 June 2015

Keywords:
Dynamic topography
Caribbean
Shallow mantle flow

ABSTRACT

The Pacific Ocean is surrounded by subduction zone systems leading to a decreasing surface area as well as sub-surface mantle domain. In contrast, the Atlantic realm is characterized by passive margins and growing in size. To maintain global mass balance, the Caribbean and the Scotia Sea have been proposed as Pacific-to-Atlantic transfer channels for sub-lithospheric shallow mantle. We concentrate on the Caribbean here and test this idea by calculating the present-day regional dynamic topography in search of a gradual decrease from west to east that mirrors the pressure gradient due to the shrinkage of the Pacific. To calculate the dynamic topography, we isostatically correct the observed topography for sediments and crustal thickness variations, and compare the result with those predicted by lithospheric cooling models. The required age-grid was derived from our recently published reconstruction model. Our results confirm previous geochemical and shear-wave splitting studies and suggest some lateral asthenosphere flow away from the Galapagos hotspot. However, they also indicate that this flow is blocked in the Central Caribbean. This observation suggests that rather than through large scale Pacific-to-Atlantic shallow mantle flow, the global mass balance is maintained through some other process, possibly related to the deep mantle underneath Africa.

1. Introduction

The conception of a relatively mobile, mostly laterally flowing asthenosphere between 100 and 400 km depth, on which tectonic plates glide easily, has been accepted for a long time [1]. Several lines of evidence are consistent with this view and comprise isostatic considerations of mountain belts (see [2] for a review), geoid and postglacial rebound studies [3,4], seismic surveys [5,6] as well as mineralogical investigations [7]. Also, numerical mantle convection models [8] and analytical fluid dynamic calculations [9] can be made consistent with a relatively weak upper mantle. In fact, it has been proposed that an asthenosphere is essential in sustaining plate tectonics on Earth [10].

This understanding of the asthenosphere has great consequences for the general perception of mantle exchange processes between the Pacific, Atlantic and Indian Ocean mantle domains, which differ from each other in their isotope and trace element chemistry [e.g. 11]. While the Pacific is shrinking, because subduction of Pacific lithosphere in the marginal subduction zones occurs faster than the creation of new lithosphere along the Pacific mid-ocean ridges, the Atlantic and Indian Oceans are growing as more lithosphere is being created than subducted. This poses the question where the underlying mantle reservoirs of the Indian and Atlantic Oceans are fed from, and where the material underneath the shrinking Pacific goes to.

To this end, Walter Alvarez [12] suggested a concept of asthenosphere exchange between the three mantle domains as a mechanism to achieve global mass balance. He viewed the Caribbean, for which a slab gap in the Costa Rica/Panama region has been suggested [13] (Fig. 1), and the Scotia Seas as gateways for Pacific-to-Atlantic asthenosphere flux. The Australian-Antarctic discordance was suggested for asthenosphere transfer between the Pacific and Indian Ocean mantle domains.

Alvarez [12] viewed these outlets as necessary, because direct lateral asthenospheric mantle flow from the closing Pacific into the opening Atlantic/Indian mantle domains is thought to be blocked by sinking slabs and deep continental roots, known as the tectosphere and reaching down to approximately 200 km depth [14], everywhere else along the Pacific Plate margin. The flow is supposedly triggered by the shrinkage of the Pacific realm, which is envisaged to cause a pressure gradient driving the asthenosphere through these proposed outlets.

* Corresponding author at: Formerly at b, now at a.
E-mail addresses: rnerlich@geophysik.uni-muenchen.de (R. Nerlich), stuart@simula.no (S.R. Clark), bunge@lmu.de (H.-P. Bunge).
[1] Tel.: +47 4745 2870; fax: +47 6782 8201.
[2] Tel.: +49 (89) 2180 4234; fax: +49 (89) 2180 4205.

http://dx.doi.org/10.1016/j.grj.2015.06.001
2214-2428/

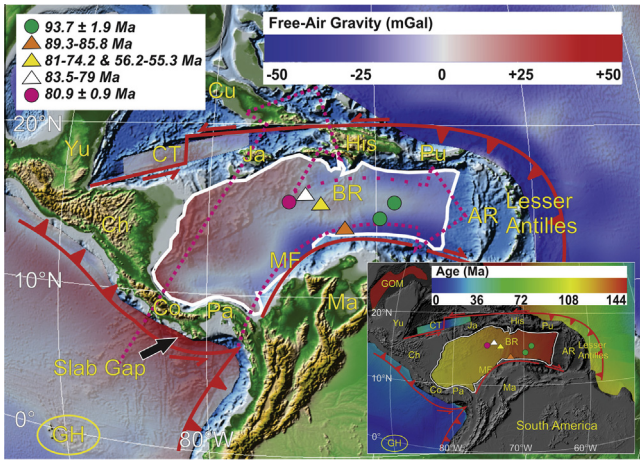

Fig. 1. (Main) Overview of the Caribbean Sea with superimposed long-wavelength free-air gravity anomalies (low-pass filtered to 5°) from Tapley et al. [18] shown in areas with age-grid coverage (topography shown in other areas). (Insert) Regional age-grid from Nerlich et al. [16], ranging in the Caribbean realm from 105 to 144 Ma. (Both) The white outline shows the region of the Caribbean large igneous plateau [19]. Asthenosphere flow paths according to Alvarez [12] are dotted in purple. The age of rock samples [20,21] drilled from basement in the region is indicated by dots (Ar/Ar dated) and triangles (dated by inclusions or overlying strata). Insert on the top left hand side shows sample age ranges. Abbreviations are as follows: Galapagos hotspot (GH), Maracaibo Block (Ma), Panama (Pa), Costa Rica (Co), Chortis Block (Ch), Yucatan Block (Yu), Jamaica (Ja), Cuba (Cu), Hispaniola (His), Puerto Rico (Pu), Gulf of Mexico (GOM), Cayman Trough (CT), Aves Ridge (AR), Beata Ridge (BR), and Magdalena Fan (MF). Note, all figures but Figs. 4 and 7 are presented using 4DPlates software [22]. (For interpretation of the references to colour in this figure legend, the reader is referred to the web version of this article.)

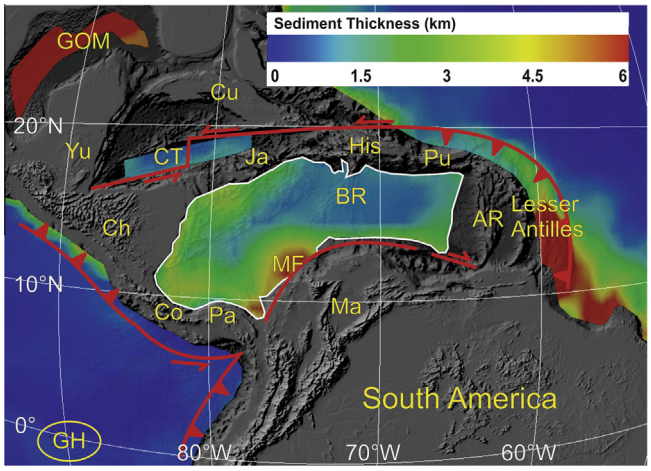

Fig. 2. Sediment distribution in the Caribbean realm based on CRUST1.0 [23]. Abbreviations are as in Fig. 1.

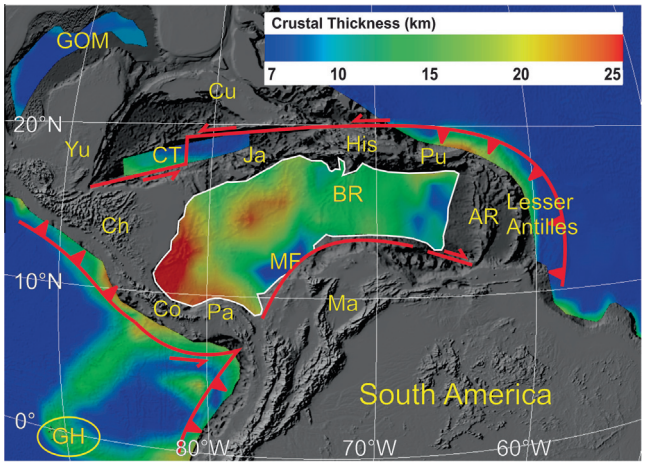

Fig. 3. Crustal thickness variations according to CRUST1.0 [23]. Abbreviations are as in Fig. 1.

We have tested Alvarez's [12] hypothesis for the Scotia Sea already [15], and focus in this paper on the Caribbean Sea (Fig. 1). We follow the conceptual view of Nerlich et al. [15] and calculate the present-day dynamic topography assuming that it is indicative of asthenospheric mantle flow. If the asthenosphere flows from the Pacific mantle domain around the northern tip of South America into the Atlantic realm, we expect a gradual decrease in dynamic topography from the Pacific realm throughout the Caribbean Sea.

2. Geological setting

A detailed outline of the Caribbean plate tectonic history may be found in our previous paper [16]. Here, only a brief overview of some of the region's features is given: At present day the northern plate boundary is characterised by transtension while the southern plate boundary by a complicated transpressional regime [17]. Subduction zones along the western Central American margin and Lesser Antilles arc form the plate boundaries on the western and eastern ends of the region (Fig. 1). In addition, there is a slab gap west of Panama and Costa Rica [13]. The relatively few sample points from Caribbean basement (Fig. 1) indicate that it was formed between ~94 and 80 Ma ago.

Positive free-air gravity anomalies of up to 30 mGal are observed in the northwest of the Caribbean Plateau as well as above the Beata Ridge, while negative anomalies of up to 45 mGal are found at the western and eastern edges of the region (Fig. 1). Relatively thin sediment cover (<2 km) is present in the northeastern part of the region around the Beata Ridge (Fig. 2), whereas the Magdalena Fan (MF, Fig. 2) has up to 6 km of sediment cover. The thickest crustal (>20 km) regions are the western section of the Plateau as well as to the northwest of the Magdalena Fan (Fig. 3). The Magdalena Fan itself and the easternmost part of the Plateau have a lower crustal thickness of up to 12 km. The remaining parts of the Plateau are between 15 and 18 km thick, i.e. more than twice as thick as typical oceanic crust.

3. Residual (dynamic) topography deconvolution methodology

Dynamic topography refers to the mantle component of the observed topography, which is due to transient viscous stresses caused by mantle up- or downwellings resulting from density variations within Earth's mantle [24]. For oceanic regions an estimate can be derived in three steps: (1) The observed bathymetry is corrected for sediments and crustal thickness variations, assuming local isostacy; (2) Based on standard cooling models [25–27] an expected basement depth can be derived, for which a precise lithospheric age distribution is essential; (3) The difference between the expected basement depth from step (2) and the isostatically corrected observed basement depth from step (1) is the 'dynamic' component of the convecting mantle [28].

For step (1), we made use of the recently released 1 × 1-degree global crustal and sediment thickness model CRUST1.0 of Laske et al. [23], see Figs. 2 and 3. The model is divided into three sediment and three crystalline crustal layers and contains density distributions for each one of them. The isostatic correction for sediments (S_c) is calculated by:

$$S_c = \left(\frac{\rho_s - \rho_w}{\rho_a - \rho_w}\right) * S_t \quad (1)$$

ρ_s, ρ_w, and ρ_a refer to the densities of the sediments, water (1019 kg/m^3), and asthenosphere (3200 kg/m^3). S_t is the total sediment thickness at each respective grid point. The sediment correction was calculated for the sediment layers separately and subtracted from the sediment loaded, observed bathymetry [29]. We excluded bathymetry that was shallower than the mean water depth minus two times the standard deviation (for the Pacific/Atlantic, we used 4 times the standard deviation in order to reflect the greater variation due to the greater polygon sizes), to avoid the inclusion of continental crust.

The isostatic correction (C_c) for the crystalline crust is given by:

$$C_c = \left(\frac{\rho_a - \rho_c}{\rho_a - \rho_w}\right) * (C_t - C_{\text{avg}}) \quad (2)$$

ρ_c and C_t indicate the density of the crust and the crustal thickness at each grid point. C_{avg} refers to the average crustal thickness of oceanic crust, which is approximately 7.1 km [30]. We calculated a weighted mean average density for all grid points (density range: 2870–2960 kg/m^3| mean value: 2950 kg/m^3) of the three crustal layers. This mean density was used in Eq. (2) to derive the isostatic crustal correction for each of the three crystalline crustal layers, which were added to the sediment corrected bathymetry.

For the calculation of a theoretical basement depth, the age distribution is usually derived from magnetic isochron interpretations. However, the thickened crust of the Caribbean Plateau prohibits the direct measurement of magnetic anomalies, such that we derived an age-grid (Fig. 1, insert) from our own plate reconstruction model [16]. The model fits the reconstructed position of the Caribbean Plateau with the paleo-position of the Galapagos hotspot at the main phase of plateau formation between ~94 and 88 Ma [20,21], indicating that the Plateau was built as a consequence of the Galapagos plume head surface arrival, consistent with geochemical studies [31–33].

The dynamic topography (DT) is finally given by the following formula:

$$DT = d_{\text{age}} - (d + S_t - S_c + C_c), \quad (3)$$

for which depths are positive downwards and d_{age} is the predicted depth. The terms in the brackets in (3) represent the observed bathymetry (d), the sediment thickness (S_t) and the two isostatic corrections from Eqs. (1) and (2).

4. Uncertainty determination

Because of the uncertainty and relatively sparse resolution of the sedimentary thickness data from CRUST1.0 with respect to the bathymetric data, we applied two approaches to evaluate the uncertainty of our approach. The first approach consists of a series of quasi-Monte Carlo simulations [34] in which we approximate the uncertainty of the dynamic topography by considering the parameters in Eqs. 1 and 2 as probabilistic rather than deterministic or discrete values. Table 1 presents the various stochastic parameters that we used in the calculation.

Table 1
Stochastic parameters used in the quasi-Monte Carlo simulation. $N(\mu, \sigma)$ is a normal distribution with mean μ and standard deviation σ, while $U(a,b)$ is a uniform distribution with upper and lower values a and b, respectively.

Parameter	Symbol	Stochastic representation	Units
Sediment density	ρ_s	$P_s \sim N$ (2200,200)	kg/m^3
Crustal density	ρ_c	$P_c \sim N$ (2950,200)	kg/m^3
Asthenospheric density	ρ_a	$P_a \sim U$ (3100,3300)	kg/m^3
Sediment thickness	z_s	$Z_s \sim N$ (z_s, 500)	m
Crustal thickness	z_c	$Z_c \sim N$ (z_c, 500)	m

The sediment and crustal density distributions in Table 1 were derived from the weighted mean and standard deviation of the three CRUST1.0 sediment and crustal layers in the domain (outlined in white in Fig. 1), respectively. To represent the uncertainty in the asthenospheric density, we used a uniform distribution centred on 3200 kg/m^3 [30]. Finally, we added 500 m of normally-distributed or white noise to the crustal and sedimentary thickness data from CRUST1.0.

For each of the distributions in Table 1, N samples were drawn using the Halton Sampling technique [35] using a Halton sequence based on prime number 2 in the interval (0, 1), dropping the first 2 numbers in the sequence. The N results of Eqs. (1) and (2) were then calculated using these sampled values as parameters to calculate the dynamic topography according to Eq. (3). The N resulting dynamic topography results were then used to calculate the sample mean and standard deviation at each point for the domain.

To determine convergence of the quasi-Monte Carlo method, the mean was calculated analytically – equivalent to using the mean of the parameters in place of the parameters in Eqs. (1)–(3). The normalised RMS error between the estimated mean from the quasi-Monte Carlo method and the analytical mean is shown in Fig. 4 as a function of N. Linear convergence in the log–log plot is achieved up to N = 10,000, while convergence is achieved at about N = 100,000 after which no significant improvement in the error is achieved with increasing N. The normalised RMS error is smaller than 0.06, corresponding to about 15 m in dynamic topography. The calculated variance of the dynamic topography, based on $N = 10^7$, is presented in Section 5.

The second method to constrain the uncertainty was to vary the lithospheric cooling model used to determine the theoretical ocean depth, since lithospheric cooling models differ from each other for the oldest ocean floor (between 100 and 150 million years old). We calculated the dynamic topography using three different models. The half-space cooling model (Hs) [25] is uniformly based on the function: basement depth = 2600 + 345 × $\sqrt{}$(age). The GDH1 [26] and PSM [27] plate models deviate from the continuous "square-root of age" assumption in that these models assume negative exponential functions for ages greater than 20 Ma and 70 Ma, respectively.

5. Results

The standard deviation of the dynamic topography from the quasi-Monte Carlo approach is presented in Fig. 5. The regions adjacent to Costa Rica show high standard deviation in the dynamic topography because of the uncertainty in the sediment and crustal densities impacting the combined larger correction for higher mean sediment and crustal thicknesses. While the mean standard deviation is 675 m, the mode, which is less sensitive to the outliers mentioned above, is 489 m and more representative of the standard deviation of dynamic topography in the Magdalena Fan and Beata Ridge (MF and BR, Fig. 6).

The calculated dynamic topography signal based on the GDH1 lithospheric cooling model is shown in Fig. 6. The figure also includes the locations of profiles visualizing the amplitude of dynamic topography (Fig. 7) based on the three tested cooling models. All profiles have their origin at the Galapagos hotspot (GH) and continue eastward through the proposed slab window and into various directions within the Caribbean realm. The diagrams visualize the discrepancy of dynamic topography predictions between the different lithospheric cooling models: While the predictions in terms of the dynamic topography amplitude for young seafloor (<60 Ma) such as for the region west of Central America in the

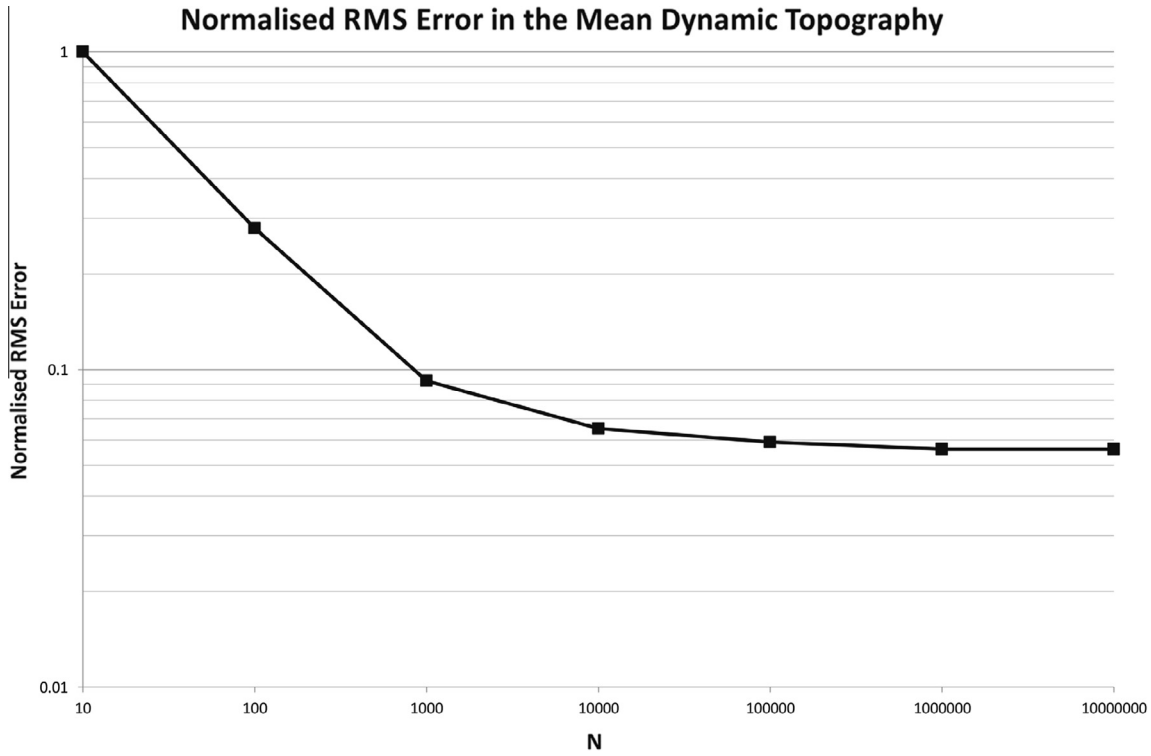

Fig. 4. Log–log plot of the normalised RMS error between the analytical mean and the estimated mean derived from the *N*th quasi-Monte Carlo iteration. The error is normalised relative to $N = 10$ for which the RMS error is 267 m.

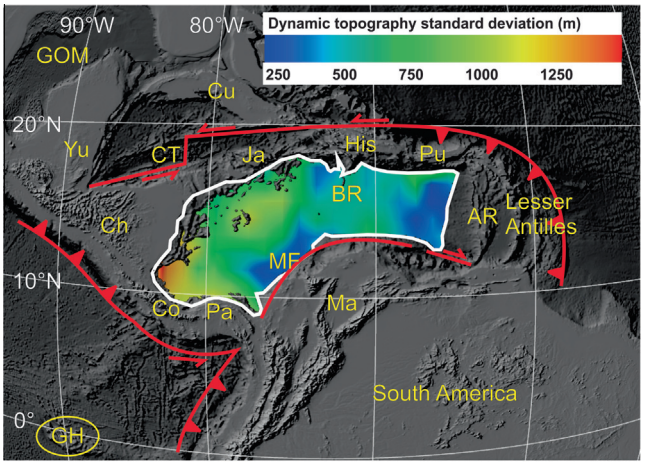

Fig. 5. Standard deviation of the dynamic topography derived from the quasi-Monte Carlo simulations, with $N = 10^7$. The mode deviation is 489 m, the median is 612 m and the mean is 675 m.

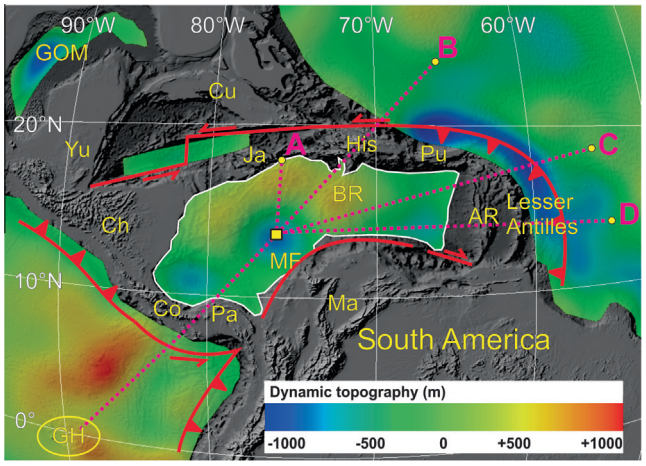

Fig. 6. Present-day bathymetry (gray-scale) with superimposed dynamic topography based on the GDH1 lithospheric cooling model [26]. Note, because dynamic topography is a long-wavelength feature, the results presented here were low-pass filtered (cut-off wavelength: 5°, i.e. ~550 km). The central part of the Caribbean Plateau (location is indicated by a yellow square) shows a regional dynamic topography low. The northern part of the region and the Beata Ridge are characterized by positive, the western and eastern ends of the region by negative dynamic topography. Locations of profiles A-D (Fig. 7) originating at GH are illustrated by dotted lines. (For interpretation of the references to colour in this figure legend, the reader is referred to the web version of this article.)

Pacific are very similar, they differ substantially in dynamic topography amplitude in the Caribbean realm, where the ocean floor is presumed to be very old (>100 Ma). However, despite these absolute amplitude differences the patterns are very similar and thus useful to infer mantle flow. Based on the GDH1 model, the calculated minimum/maximum dynamic topography signals of the outlined Caribbean Plateau are −560 /+760 m (half-space model: −183/+1390 m; PSM model: −450/+920 m). The largest positive signal is observed around the Beata Ridge and southeast of Jamaica. The largest negative signal is located north of the Magdalena Fan (GDH1: ~−750 m). Additionally, two dynamic topography lows are located at the western and eastern ends of the Caribbean Plateau. The Galapagos hotspot in the Pacific realm is characterized by positive dynamic topography of ~500 m (according to all cooling models), leading to a relative difference between the dynamic topography low north of the Magdalena Fan and the hotspot of ~1250 m (Fig. 7, based on GDH1). Finally, a local maximum is observed just to the east of Panama (Fig. 7).

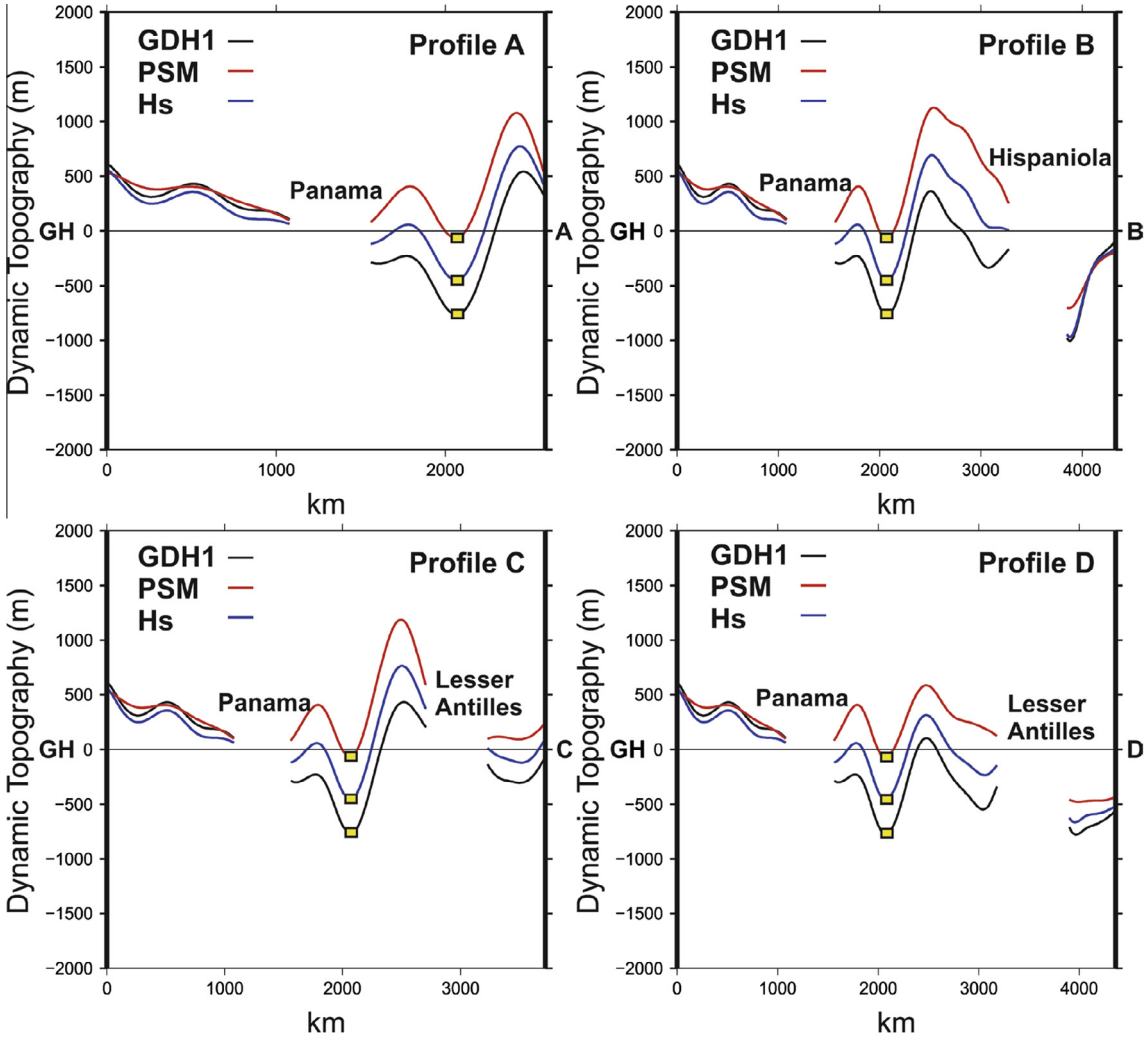

Fig. 7. Dynamic topography based on three different lithospheric cooling models along the profiles shown in Fig. 6: (1) GDH1 [26] in black, (2) PSM [27] in red, and (3) Hs [25] in blue. The three models lead to similar patterns but differ in the predicted dynamic topography amplitude. The yellow rectangle corresponds to the position of the central dynamic topography low in the Caribbean Sea (see Fig. 6). Note the decrease in dynamic topography from west to east away from the Galapagos hotspot towards the central part of the Caribbean. Note also the dynamic topography increase in all directions past this Central Caribbean dynamic topography low. (For interpretation of the references to colour in this figure legend, the reader is referred to the web version of this article.)

6. Discussion

Regional geochemical variations along the Central American Arc have been known for a long time and been linked to different mantle sources [36,37]: While rocks from Nicaragua and Guatemala are associated with a slab-metasomatized, mid-ocean ridge basalt (MORB)-source mantle, rocks from Costa Rica and Panama, which are little affected by subduction metasomatism, indicate an ocean-island basalt (OIB)-type enriched mantle origin. Additionally, a striking similarity of the rocks found in Costa Rica and Panama with those from the Galapagos Islands has been noticed [13,38]. Shallow mantle flow away from the Galapagos hotspot through a seismically quiet zone related to a slab gap between the subducting Cocos and Nazca plates into the Caribbean realm was suggested by these authors as a mechanism to explain the geochemical variations along the Central American Arc. Alternatively, it was argued that variations in the incoming plate's geometry as well as in the composition and fluid content could be responsible for the chemical differences [39].

Support for the mantle flow hypothesis comes from several shear-wave splitting studies, which measure the lattice preferred orientation of olivine crystals in the upper mantle [40–44]. These studies indicated the presence of a regional west-east oriented asthenosphere flow underneath the Caribbean Sea. Yet, these studies were mostly limited to the northeastern margin of South America and the Lesser Antilles arc, rather than Panama and Costa Rica. The only measurement just north of the proposed slab gap (Fig. 1) indicated trench parallel flow [42]. Also, it should be noted that relative flow directions in general cannot be estimated from shear-wave splitting measurements but merely the orientation.

Compared to geochemical and shear-wave splitting studies, our approach offers a broader sense of the regional asthenosphere flow. The profiles shown in Fig. 7 indicate a decreasing dynamic topography signal away from the Galapagos hotspot towards the proposed slab gap and into the Caribbean realm. This observation indicates shallow mantle inflow from the Pacific into the Caribbean realm and confirms the above mentioned studies and Alvarez [12] mantle flow hypothesis. Undulations along the profiles are observable; foremost the dynamic topography high east of Panama stands in contrast to the general trend. However, the amplitude of this dynamic topography high is strongly model-dependent and most prominent using the PSM model and almost negligible according to the GDH1 model (Fig. 7).

Furthermore, the region east of Panama shows rather high variance, whereas the low in the Central Caribbean is a relatively robust feature (Fig. 5). This also applies to the dynamic topography high around the Galapagos hotspot, where the age-grid is derived from magnetic isochrons and the seafloor is young, leading to almost identical predictions of all tested lithospheric cooling models.

Additionally, it is noticeable that the profiles of Fig. 7 show a relatively large positive dynamic topography signal in all directions past the dynamic topography low in the Central Caribbean (Fig. 6). This suggests that only a tongue of Pacific derived asthenosphere has reached the Central Caribbean realm, where the flow is blocked, possibly by the subducting Lesser Antilles slab. If true, an upward reflection of the flow could perhaps cause the observed positive dynamic topography signals further to the east and north of the central dynamic topography low. The negative signal observed on the eastern edge of the Caribbean Plateau most likely reflects the sinking slab of the Lesser Antilles subduction zone. Similarly, the negative signal east of Costa Rica may be related to the subducting Cocos Plate slab. However, it could also be due to a regional over prediction of the crustal thickness in the CRUST1.0 model [23], which is well above 20 km in this area (Fig. 3).

Finally, it is noteworthy that our dynamic topography amplitudes are all in the commonly accepted range of ±1000 m [24] (except the maximum positive dynamic topography signal predicted by the half-space cooling model). A quantitative comparison of our dynamic topography results (Fig. 6) with the regional long-wavelength free-air gravity signal (Fig. 1) shows a weak positive correlation ($r = 0.4$). This is in broad agreement with the global results of Winterbourne et al. [30]. Both of these results suggest that the derived age distribution and our dynamic topography results are reasonable.

Despite some potential, most likely Galapagos plume-derived inflow into the Caribbean realm, the absence of a gradual decreasing dynamic topography signal from west to east throughout the entire Caribbean region indicates the absence of a continuous flow into the Atlantic mantle domain. It seems unlikely that the growing Atlantic mantle reservoir is compensated through shallow mantle inflow through the Caribbean realm alone. We arrived at the same conclusion for the Scotia Sea [15], and suggest that the deep mantle beneath Africa is a far more likely primary source to supply the growing Atlantic mantle reservoir. The elevated topography of the African superswell [45], which is inferred to be due to a deep mantle upwelling [46], contrasts with significant negative dynamic topography of up to ~1 km at the conjugate South American margin in the Argentine Basin [e.g., 30,47,48] as well as with wide areas northeast off the northern margin of Brazil (Guyana Basin). These topography lows are possibly related to the subduction of the former Phoenix and Farallon plates that nowadays reside in the lower mantle [49]. The remarkable dynamic topography gradient across the entire South Atlantic is consistent with westward flow emanating from the African superplume [48,50,51]. It is likely that this large scale flow has more relevance compared to regional inflow through the Caribbean or Scotia Sea in the process of establishing mass balance between the Pacific and Atlantic mantle reservoirs.

Acknowledgments

The presented work was funded by a research grant from Statoil AS. The authors thank Statoil AS and Kalkulo AS for the use of 4DPlates. HPB acknowledges funding from the DFG SAMPLE SPP. We also thank editor Scott King as well as the reviewers Graeme Eagles and Rhodri Davies for their help and constructive comments.

References

[1] Chase CG. Asthenospheric counterflow: a kinematic model. Geophys J Roy Astron Soc 1979;56:1–18.
[2] Watts AB. Isostasy and flexure of the lithosphere. 1st ed. Cambridge, UK: Cambridge University Press; 2001.
[3] Hager BH, Richards MA. Long-wavelength variations in Earths geoid – physical models and dynamical implications. Philos Trans R Soc Lond 1989;328:309–27.
[4] Mitrovica JX. Haskell [1935] revisited. J Geophys Res Solid Earth 1996;101:555–69. http://dx.doi.org/10.1029/95JB03208.
[5] Grand SP, Helmberger DV. Upper mantle shear structure of North America. Geophys J Roy Astron Soc 1984;76:399–438.
[6] Debayle E, Kennett B, Priestley K. Global azimuthal seismic anisotropy and the unique plate-motion deformation of Australia. Nature 2005;433:509–12. http://dx.doi.org/10.1038/nature03247.
[7] Stixrude LP, Lithgow-Bertelloni C. Mineralogy and elasticity of the oceanic upper mantle: origin of the low-velocity zone. J Geophys Res 2005;110. http://dx.doi.org/10.1029/2004JB002965.
[8] Bunge H-P, Richards MA, Baumgardner JR. Effect of depth-dependent viscosity on the planform of mantle convection. Nature 1996;379:436–8. http://dx.doi.org/10.1038/379436a0.
[9] Busse FH, Richards MA, Lenardic A. A simple model of high Prandtl and high Rayleigh number convection bounded by thin low-viscosity layers. Geophys J Int 2006;164:160–7. http://dx.doi.org/10.1111/j.1365-246X.2005.02836.x.
[10] Richards MA, Yang W-S, Baumgardner JR, Bunge H-P. Role of a low- viscosity zone in stabilizing plate tectonics: implications for comparative terrestrial planetology. Geochem Geophys Geosyst 2001;2. http://dx.doi.org/10.1029/2000GC000115.
[11] Schiano P, Birck J-L, Allegre CJ. Osmium-strontium-neodymium-lead isotopic covariations in mid-ocean ridge basalt glasses and the heterogeneity of the upper mantle. Earth Planet Sci Lett 1997;150:363–79. http://dx.doi.org/10.1016/S0012-821X(97)00098-8.
[12] Alvarez W. Geological evidence for the geographical pattern of mantle return-flow and the driving mechanism of plate-tectonics. J Geophys Res 1982;87:6697–710. http://dx.doi.org/10.1029/JB087iB08p06697.
[13] Johntson ST, Thorkelson DJ. Cocos-Nazca slab window beneath Central America. Earth Planet Sci Lett 1997;146:465–74. http://dx.doi.org/10.1016/S0012- 821X(96)00242-7.
[14] Jordan TH. Composition and development of continental tectosphere. Nature 1978;274:544–8. http://dx.doi.org/10.1038/274544a0.
[15] Nerlich R, Clark SR, Bunge H-P. The Scotia Sea gateway: no outlet for Pacific mantle. Tectonophysics 2013;604:41–50. http://dx.doi.org/10.1016/j.tecto.2012.08.023.
[16] Nerlich R, Clark SR, Bunge H-P. Reconstructing the link between the Galapagos hotspot and the Caribbean Plateau. GeoResJ 2014;1–2:1–7. http://dx.doi.org/10.1016/j.grj.2014.02.001.
[17] van der Lelij R, Spikings RA, Kerr AC, Kounov A, Cosca M, Chew D, Villagomez D. Thermochronology and tectonics of the Leeward Antilles: Evolution of the southern Caribbean Plate boundary zone. Tectonics 2010;29. http://dx.doi.org/10.1029/2009TC002654.
[18] Tapley B, Ries J, Bettadour S, Chambers D, Cheng M, Condi F, Gunter B, Kang Z, Nagel P, Pastor R, Pekker T, Poole S, Wang F. GGM02 – an improved Earth gravity field model from GRACE. J Geod 2005;79:467–78. http://dx.doi.org/10.1007/s00190-005- 0480-z.
[19] Mauffret A, Leroy S, Vila JM, Hallot E, de Lepinay BM, Duncan RA. Prolonged magmatic and tectonic development of the Caribbean Igneous Province revealed by a diving submersible survey. Marine Geophys Res 2001;22:17–45. doi: 10.1023/a:1004873905885.
[20] Kerr AC, Pearson DG, Nowell GM. Magma source evolution beneath the Caribbean oceanic plateau: new insights from elemental and Sr-Nd-Pb-Hf isotopic studies of ODP Leg 165 Site 1001 basalts: Geological Society of London Special Publications 2009;328:809–827. doi: 10.1144/sp328.31.
[21] Hastie AR, Mitchell SF, Treloar P, Kerr AC, Neill I, Barfod DN. Geochemical components in a Cretaceous island arc: The Th/La-$(Ce/Ce*)_{Nd}$ diagram and implications for subduction initiation in the inter-American region. Lithos 2013:57–69. doi: 10.1016/j.lithos.2012.12.001.
[22] Clark SR, Skogseid J, Smethrust M, Tarrou C, Stensby TV, Bruaset AM, Thurmond AK. On the fly visualization of multilayer geoscientific datasets using 4DPlates. Comput Geosci 2012;47:46–51. http://dx.doi.org/10.1016/j.cageo.2012.03.015.
[23] Laske G, Masters G, Ma Z, Pasyanos M. Update on CRUST1.0 – A 1-degree Global Model of Earth's Crust, Geophysical Research Abstracts, 15, Abstract EGU2013-2658; 2013.
[24] Braun J. The many surface expressions of mantle dynamics. Nat Geosci 2010;3:825–33. http://dx.doi.org/10.1038/ngeo1020.
[25] Turcotte DL, Oxburgh ER. Finite amplitude convective cells and continental drift. J Fluid Mech 1967;28:29–42. http://dx.doi.org/10.1017/S0022112067001880.
[26] Stein CA, Stein S. A model for the global variation in oceanic depth and heat-flow with lithospheric age. Nature 1992;359:123–9. http://dx.doi.org/10.1038/359123a0.
[27] Parsons B, Sclater JG. Analysis of variation of ocean floor bathymetry and heat-flow with age. J Geophys Res 1977;82:803–27. http://dx.doi.org/10.1029/JB082i005p00803.

[28] Kido M, Seno T. Dynamic topography compared with residual depth anomalies in oceans and implications for age-depth curves. Geophys Res Lett 1994;21:717–20. http://dx.doi.org/10.1029/94GL00305.
[29] Amante C, Eakins BW. ETOPO 1 arc-minute global relief model: Procedures, data sources and analysis. NOAA technical memorandum NESDIS NGDC-24; 2009.
[30] Winterbourne J, Crosby A, White N. Depth, age and dynamic topography of oceanic lithosphere beneath heavily sedimented Atlantic margins. Earth Planet Sci Lett 2009;287:137–51. http://dx.doi.org/10.1016/j.epsl.2009.08.019.
[31] Hauff F, Hoernle K, Schmincke HU, Werner R. A mid Cretaceous origin for the Galapagos hotspot: volcanological, petrological and geochemical evidence from Costa Rican oceanic crustal segments. Geol Rundsch 1997;86:141–55. http://dx.doi.org/10.1007/pl00009938.
[32] Geldmacher J, Hanan BB, Blichert-Toft J, Harpp K, Hoernle K, Hauff F, Werner R, Kerr AC. Hafnium isotopic variations in volcanic rocks from the Caribbean Large Igneous Province and Galapagos hot spot tracks. Geochem Geophys Geosyst 2003;4. http://dx.doi.org/10.1029/2002GC000477.
[33] Thompson PME, Kempton PD, White RV, Kerr AC, Tarney J, Saunders AD, Fitton JG, McBirney A. Hf-Nd isotope constraints on the origin of the Cretaceous Caribbean plateau and its relationship to the Galapagos plume. Earth Planet Sci Lett 2003;217:59–75. http://dx.doi.org/10.1016/S0012-821X(03)00542-9.
[34] Kroese DP, Taimre T, Botev ZI. Handbook of Monte Carlo Methods. Hoboken, NJ: John Wiley & Sons, Inc.; 2011. http://dx.doi.org/10.1002/9781118014967.
[35] Feinberg J, Clark SR. RoseDist: Generalized Tool for Simulating with Non-Standard Probability Distributions, 20th International Congress on Modelling and Simulation, Adelaide, Australia, 1–6 December; 2013.
[36] Carr MJ. Symmetrical and segmented variation of physical and geochemical characteristics of the Central American volcanic front. J Volcanol Geoth Res 1984;20:231–52. http://dx.doi.org/10.1016/0377-0273(84)90041-6.
[37] Herrstrom EA, Reagan MK, Morris JD. Variation in lava composition associated with flow of asthenosphere beneath southern Central America. Geology 1995;23:617–20. http://dx.doi.org/10.1130/0091-7613(1995)023<0617:VILCAW>2.3.CO;2.
[38] Abratis M, Wörner G. Ridge collision, slab-window formation, and the flux of Pacific asthenosphere into the Caribbean realm. Geology 2001;29:127–30. http://dx.doi.org/10.1130/0091-7613(2001)029<0127:RCSWFA>2.0.CO;2.
[39] Rüpke LH, Morgan JP, Hort M, Conolly JAD. Are the regional variations in Central American arc lavas due to differing basaltic versus peridotitic slab sources of fluids? Geology 2002;30:1035–8. http://dx.doi.org/10.1130/0091-7613(2002)030<1035:ATRVIC>2.0.CO;2.
[40] Russo RM, Silver PG. Trench-parallel flow beneath the Nazca Plate from Seismic Anisotropy. Science 1994;263:1105–11. http://dx.doi.org/10.1126/science.263.5150.1105.
[41] Russo RM, Silver PG, Franke M, Ambeh WB, James DE. Shear-wave splitting in northeast Venezuela, Trinidad, and the eastern Caribbean. Phys Earth Planet Inter 1996;95:251–75. http://dx.doi.org/10.1016/0031-9201(95)03128-6.
[42] Pinero-Feliciangeli LT, Kendall J-M. Sub-slab mantle flow parallel to the Caribbean plate boundaries: inferences from SKS splitting. Tectonophysics 2008;462:22–34. http://dx.doi.org/10.1016/j.tecto.2008.01.022.
[43] Growdon MA, Pavlis GL, Niu F, Vemon FL, Rendon H. Constraints on mantle flow at the Caribbean-South American plate boundary inferred from shear wave splitting. J Geophys Res 2009;114:B02303. http://dx.doi.org/10.1029/2008JB005887.
[44] Masy J, Niu F, Levander A, Schmitz M. Mantle flow beneath northwestern Venezuela: Seismic evidence for a dep origin of the Merida Andes. Earth Planet Sci Lett 2011;305:396–404. http://dx.doi.org/10.1016/j.epsl.2011.03.024.
[45] Nyblade AA, Robinson SW. The African Superswell. Geophys Res Lett 1994;21:765–8. http://dx.doi.org/10.1029/94GL00631.
[46] Lithgow-Bertelloni C, Silver PG. Dynamic topography, plate driving forces and the African superswell. Nature 1998;395:269–72. http://dx.doi.org/10.1038/26212.
[47] Shephard GE, Liu L, Müller RD, Gurnis M. Dynamic topography and anomalously negative residual depth of the Argentine Basin. Gondwana Res 2012;22:658–63. http://dx.doi.org/10.1016/j.gr.2011.12.005.
[48] Colli L, Stotz I, Bunge H-P, Smethurst M, Clark SR, Iaffaldano G, Tassara A, Guillocheau F, Bianchi MC. Rapid South Atlantic spreading changes and coeval vertical motion in surrounding continents: evidence for temporal changes of pressure-driven upper mantle flow. Tectonics 2014;33:1304–21. http://dx.doi.org/10.1002/2014TC003612.
[49] Bunge H-P, Grand SP. Mesozoic plate-motion history below the northeast Pacific Ocean from seismic images of the subducted Farallon slab. Nature 2000;405:337–40. http://dx.doi.org/10.1038/35012586.
[50] Behn MD, Conrad CP, Silver PG. Detection of upper mantle flow associated with the African Superplume. Earth Planet Sci Lett 2004;224:259–74. http://dx.doi.org/10.1016/j.epsl.2004.05.026.
[51] Husson L, Conrad CP, Faccenna C. Plate motions, Andean orogeny, and volcanism above the South Atlantic convection cell. Earth Planet Sci Lett 2012;317–318:126–35. http://dx.doi.org/10.1016/j.epsl2011.11.040.